Phenomenological modeling of ferromagnetic shape memory alloys

Björn Kiefer[a] and Dimitris C. Lagoudas[a]

[a] Department of Aerospace Engineering, Texas A&M University, H. R. Bright Building 3141 TAMU, College Station, TX 77843-3141 USA

ABSTRACT

A thermodynamically consistent phenomenological model is presented which captures the ferromagnetic shape memory effect, i. e. the large macroscopically observable shape change of magnetic shape memory materials under the application of external magnetic fields. In its most general form the model includes the influence of the microstructure for both the volume fraction of different martensitic variants and magnetic domains on the described macroscopic constitutive behavior. A phase diagram based approach is taken to postulate functions governing the onset and termination of the reorientation process. A numerical example is given for an experiment on a NiMnGa single crystal specimen reported in the literature, for which the model is reduced to a two-dimensional case of an assumed magnetic domain structure.

Keywords: magnetic shape memory alloys, ferromagnetic shape memory effect, magnetic field induced strain, martensitic variant reorientation, phenomenological constitutive model, stress/magnetic field phase diagram, electromagnetic continuum.

1. INTRODUCTION TO MAGNETIC SHAPE MEMORY ALLOYS

Magnetic Shape Memory Alloys (MSMA) are a recent addition to the class of active materials that have attracted a lot of research interest. The most commonly studied alloys are NiMnGa and FePd. However, additional material systems, such as CoNiAl, are being investigated which show promise of superior properties to those mentioned before.[1] All of these materials exhibit thermoelastic phase transitions and therefore show conventional shape memory behavior in addition to the magnetic shape memory behavior. Although the influence of the externally applied magnetic field on the transformation temperatures as well as the phase transformation under such fields have been investigated,[2] the most striking feature of MSMA is the possibility of inducing reorientation of martensitic variants with external magnetic fields to produce large inelastic strains of $6-10\%$ in single crystals.

An experiment first presented by Tickle and James[3,4] illustrates the magnetic shape memory effect particularly well. Consider the typical strain vs. magnetic field behavior that is observed in experiments on NiMnGa single crystals as shown in Figure 1. Several aspects of the non-linear macroscopic material response are striking, such as the large strain, the considerable hysteresis under both positive and negative magnetic fields and the stress dependence of the maximum strain. The existence of threshold values for the start and end of the non-linear response regions are also apparent.

In order to explain the macroscopic behavior, one needs to understand the microstructural changes that occur inside the material. To this end, let us first consider the experimental setup schematically shown in Figure 2(a) through which the presented data was obtained. The starting point of the experiment is a single variant martensite state of the NiMnGa single crystal which is obtained by cooling and the application of an axial biasing stress. The applied stress energetically favors the tetragonal variant 1 (cf. Figure 2(b)). Figure 2(a) shows the direction of the magnetization (arrows) and 180° domain walls (horizontal lines) within the martensitic specimen. This idealized arrangement of the magnetic microstructure forms due to the fact that the magnetization of each unit cell of variant 1 is oriented along the short magnetic easy axis c and the necessity of having zero net magnetization of the material in the absence of an external magnetic field. Application of a transverse magnetic field will change

Further author information:
Contact Email: lagoudas@aero.tamu.edu

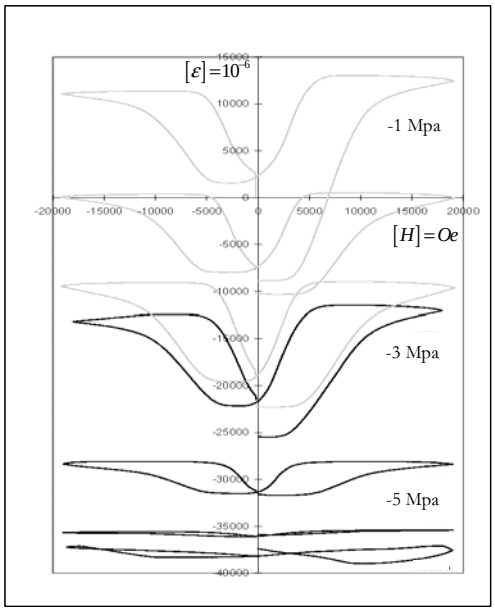

Figure 1. Strain vs. magnetic field behavior of NiMnGa single crystal specimen under different constant stress levels as reported by Tickle.[4, 5]

the variant distribution and the magnetic domain structure if a threshold value of the magnetic field is exceeded, causing the non-linear macroscopic response. The magnetic field promotes the nucleation of martensite variant 2 because of its magnetization in the y-direction. The microstructure of this intermediate state is depicted in Figure 2(c).* At large enough magnetic fields the reorientation process is complete and the specimen consists solely of variant 2 martensite. It is evident from the macroscopic behavior that further increase of the magnetic field does not result in additional straining of the material.

The physical phenomena of the magnetic shape memory behavior have now been introduced. As mentioned, the variant reorientation process and the associated macroscopic constitutive response are the focus of this paper. Section 2 discusses models available in the literature and the assumptions that are made for the model introduced in this paper. After the presentation of the model in Sections 3 and 4, the subsequent sections contain the application of the model to a specific numerical example that illustrates the applicability of the model.

2. MODELING OF MAGNETIC SHAPE MEMORY ALLOYS

2.1. Literature on modeling of the reorientation process in MSMA

Experimentally, the ferromagnetic shape memory effect (FSME) was first reported by Ullakko et. al..[6] Several groups have proposed models capturing the effect. Most of them rely on the minimization of the free energy of the system for a given magnetic, mechanical and thermal load. The model presented by James and Wuttig[7] is based on a "constraint theory of micromagnetics" (cf. DeSimone and James[8, 9]). The microstructure and the resulting macroscopic strain and magnetization response are predicted by finding the energy minimizing crystallographic configuration. Terms contributing to the free energy in their model are the Zeeman energy, the magnetostatic energy and the elastic energy. It is shown that mechanical compatibility of the microstructure implies magnetic compatibility at large strains. Hysteresis effects associated with the evolution of the microstructure are not directly accounted for in this approach. O'Handley[10] proposed a two-dimensional model in which the local

*Note that this graphic assumes a high enough magnetic anisotropy energy of the material so that the magnetization of each unit cell is fixed to the magnetic easy axis because of the energetic expense associated with the rotation of the magnetization away from it. Refer to Section 6 for a more detailed discussion of this assumption.

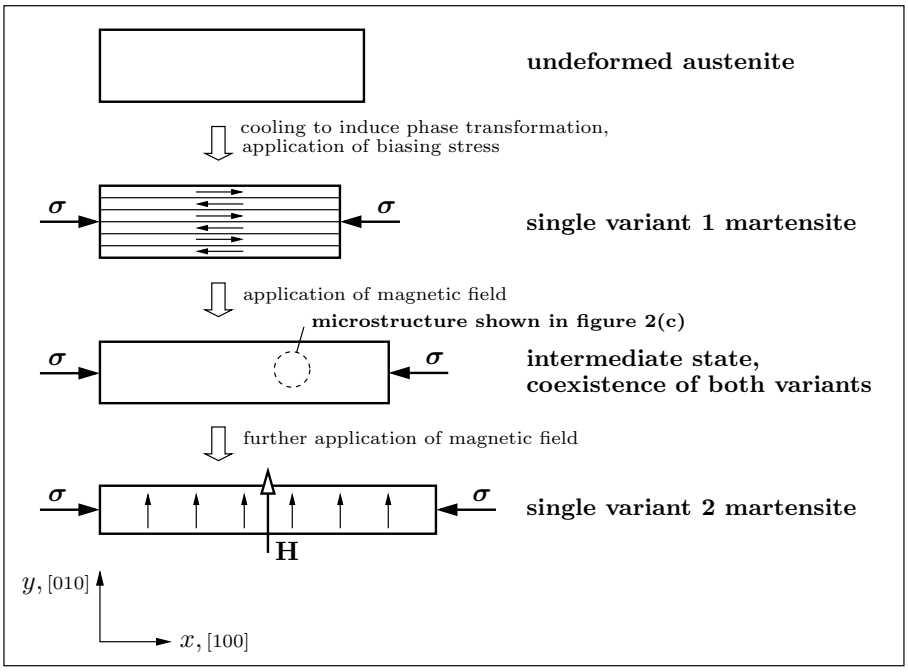

(a) Schematic of experimental setup used for the NiMnGa single crystal measurements of axial strain vs. transverse magnetic field starting from a single martensitic variant state (cf. Tickle[3, 4]).

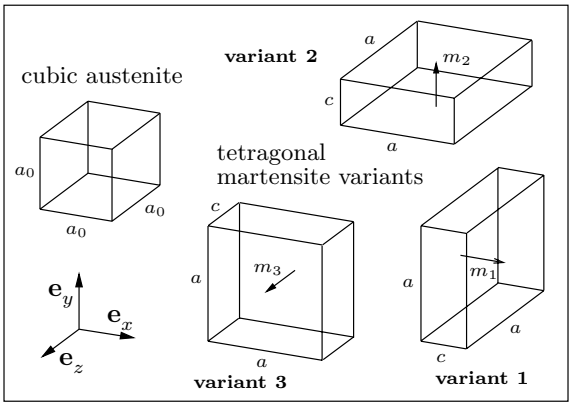

(b) Crystal structure of the austenite phase and the martensite variants. The magnetization per unit volume within each martensitic unit cell in denoted m_i.

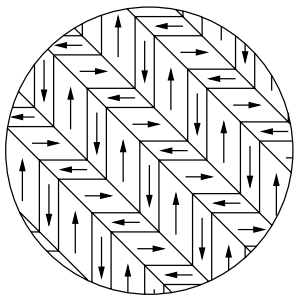

(c) Martensitic variant and magnetic domain structure at intermediate applied magnetic fields.

Figure 2.

magnetization is not necessarily constrained to the crystallographic easy axis. Depending on the magnitude of the magnetic anisotropy, either the magnetic anisotropy difference (low magnetic anisotropy case) or the Zeeman energy (high magnetic anisotropy case) are identified as the driving force for twin boundary motion in his ap-

proach. The model is able to qualitatively predict the main features of the ferromagnetic shape memory effect. The assumption is made that each twin band consists of a single magnetic domain. Buchelnikov and Bosko[11] used a free energy minimization technique in which a statistical prediction for the transition probability is utilized. Likhachev and Ullakko[12] presented a model which identifies the magnetic anisotropy energy difference as the main driving force for the reorientation process. They argue that, regardless of the physical nature of the driving force, twin boundary motion should be initiated at equivalent levels of loading. Therefore, experimentally obtained detwinning-under-stress data could be used to predict the reorientation process under the application of external magnetic fields. Hirsinger and Lexcellent[13] introduced the outline of a rate-independent phenomenological constitutive model with internal variables, in which the microstructure motivates the construction of the free energy expression, an approach that is followed in this paper as well.

2.2. Assumptions of the modeling approach

In order to be able to solve boundary value problems for MSMA continua, either analytically or with numerical methods, it is desirable to formulate a model which uses physical quantities that are easily connected to conservation laws, Maxwell's equations and continuum thermodynamics. The phenomenological model presented here is based on the development of a thermo-magneto-mechanically consistent framework (cf. Section 3). Dissipative effects such as the associated hysteresis in the variant reorientation process are taken into account by introducing internal state variables.[14] The rate independent nature of the model gives rise to reorientation functions which define critical values of the thermodynamic driving forces that govern the start and finish of the reorientation process. The evolution of the internal state variables is proposed to be based on the assumption of maximum dissipation. The specific choice of the set of internal variables is motivated by the microstructural considerations that were discussed in the introduction.

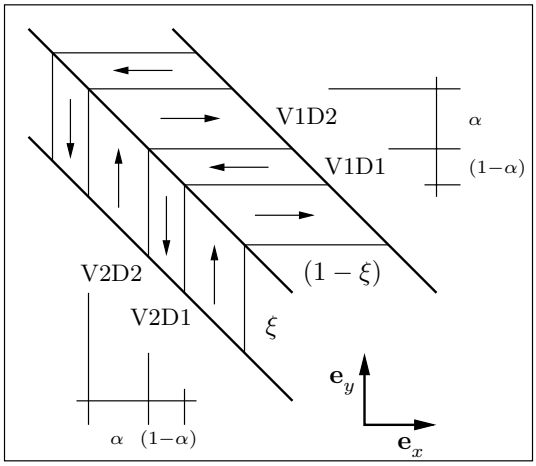

Figure 3. Coexistence of martensitic variants and magnetic domains at a twin boundary during the reorientation process.

Figure 3 shows a simplified magnification of the possible arrangement of the microstructure which was presented in Figure 1 at an intermediate magnetic load level where both variants and the magnetic domains coexist. It also introduces a nomenclature for the observed variant and domain combinations. Recall that for the sake of simplicity and feasibility of the modeling process it is assumed that the magnetic anisotropy energy is high enough to completely suppress a possible rotation of the local magnetization away from the easy axis. This particular configuration, proposed for example by Lexcellent,[13] can be regarded as a generalization of the two variant setup neglecting the magnetic domain structure.[†] The internal variables are selected to be the volume fraction of martensite variant 2, denoted ξ, the irreversible reorientation strain $\boldsymbol{\varepsilon}^{\mathrm{r}}$ and the magnetic domain 2 volume fraction α. These variables capture the characteristics of the microstructure of the material, whose

[†]Different microstructures involving more then one magnetic domain volume fraction are presently the subject of discussion but they will not be investigated further in this paper.

evolution governs the evolution of the macroscopic magnetization and the strain with applied magnetic field and stress. Furthermore, stresses are assumed to be purely mechanical in nature. This paper focuses on the formulation of a constitutive model, and not directly on the solution of specific magneto-mechanical boundary value problems. Therefore the magnetic field $\mathbf{H}$ is considered a known quantity at a particular material point and is assumed to be identical to the externally applied field for the considered problem.

Many of the discussed assumptions are standard assumptions made in the literature on modeling MSMA. As the results presented in this paper illustrate, many of the basic phenomena of these materials related to the evolution of strain with the variation of the magnetic field can be predicted quite well even with this somewhat idealized view of the underlying physics.

3. THERMO-MAGNETO-MECHANICAL FRAMEWORK FOR THE PHENOMENOLOGICAL MODELING OF MAGNETIC CONTINUA

The thermodynamic state of the material body is assumed to be captured by the Gibbs free energy function G, which depends on the independent state variables temperature T, the Cauchy stress tensor $\boldsymbol{\sigma}$ and the magnetic field $\mathbf{H}$ as well as the introduced set of internal state variables. The Gibbs free energy is related to the internal energy $u = \hat{u}(s, \boldsymbol{\varepsilon}^{\mathrm{te}}, \mathbf{M}, \xi, \boldsymbol{\varepsilon}^{\mathrm{r}}, \alpha)$ through the Legendre transformation

$$G = \hat{G}(T, \boldsymbol{\sigma}, \mathbf{H}, \xi, \boldsymbol{\varepsilon}^{\mathrm{r}}, \alpha) = u - sT - \frac{1}{\rho}\,\boldsymbol{\sigma} : \boldsymbol{\varepsilon}^{\mathrm{te}} - \frac{\mu_0}{\rho}\,\mathbf{H}\cdot\mathbf{M}\,, \tag{1}$$

where s is the specific entropy, ρ is the mass density, $\boldsymbol{\varepsilon}^{\mathrm{te}}$ the thermoelastic strain tensor, μ_0 the permeability of free space and $\mathbf{M}$ the magnetization vector. Here it has been assumed that the additive decomposition of the strain

$$\boldsymbol{\varepsilon} = \boldsymbol{\varepsilon}^{\mathrm{te}} + \boldsymbol{\varepsilon}^{\mathrm{r}} + \boldsymbol{\varepsilon}^{\mathrm{d}}\,, \tag{2}$$

is appropriate. The irreversible part of the total strain consists of the detwinning strain $\boldsymbol{\varepsilon}^{\mathrm{d}}$ and the reorientation strain $\boldsymbol{\varepsilon}^{\mathrm{r}}$. We define the detwinning strain to be related to the shape change that occurs when the material is deformed from the self-accomodated martensite state into the single variant configuration. It is assumed to be a known constant for the considered experiment. There is no additional macroscopic shape change associated with the stress free phase transformation from austenite to martensite.

The conservation of energy is expressed in the *first law of thermodynamics*, which in the strong form is given by

$$\rho\dot{u} = \boldsymbol{\sigma} : \dot{\boldsymbol{\varepsilon}} - \mathrm{div}\mathbf{q} + \rho r^{\mathrm{h}} + \frac{\mu_0}{\rho}\,\mathbf{H}\cdot\dot{\mathbf{M}}\,, \tag{3}$$

with $\mathbf{q}$ denoting the heat flux vector and r^{h} a heat source. Furthermore, a limitation on the direction in which a process can be carried out in a physical system is given by the *second law of thermodynamics* (strong form), which can be formulated in terms of the internal energy production rate γ as

$$\gamma := \dot{s} - \frac{r^{\mathrm{h}}}{T} + \frac{1}{\rho T}\,\mathrm{div}\mathbf{q} - \frac{1}{\rho T^2}\,\mathbf{q}\cdot\nabla T \geq 0\,. \tag{4}$$

Following the well-known *Coleman and Noll procedure*[15] in utilizing equations (1), (3) and (4) one derives the following constitutive implications on the dependent variables

$$\begin{aligned} \boldsymbol{\varepsilon}^{\mathrm{te}} &= -\rho\frac{\partial G}{\partial \boldsymbol{\sigma}}\;; \qquad \boldsymbol{\varepsilon} = \boldsymbol{\varepsilon}^{\mathrm{te}} + \boldsymbol{\varepsilon}^{\mathrm{r}} + \boldsymbol{\varepsilon}^{\mathrm{d}}\;; \\ s &= -\frac{\partial G}{\partial T}\;; \qquad \mu_0\mathbf{M} = -\rho\frac{\partial G}{\partial \mathbf{H}}\;. \end{aligned} \tag{5}$$

And, with the definition of the effective stress

$$\boldsymbol{\sigma}^{\mathrm{eff}} := \boldsymbol{\sigma} - \rho\frac{\partial G}{\partial \boldsymbol{\varepsilon}^{\mathrm{r}}}\;, \tag{6}$$

the Clausius-Duhem inequality takes the following form

$$\boldsymbol{\sigma}^{\text{eff}}:\dot{\boldsymbol{\varepsilon}}^{\text{r}} - \rho\frac{\partial G}{\partial \xi}\,\dot{\xi} - \rho\frac{\partial G}{\partial \alpha}\,\dot{\alpha} - \frac{1}{T}\,\mathbf{q}\cdot\nabla T \geq 0\,. \tag{7}$$

4. INCORPORATION OF MSMA CONSTITUTIVE RESPONSE

With the thermodynamic foundation of the modeling process established, one can introduce various forms of the Gibbs free energy in order to capture the desired material response. The reorientation of martensitic variants under the application of an external magnetic field, starting from a stress biased single variant martensite state, is considered here.

4.1. A specific choice of the Gibbs free energy

Under the assumptions made, the local magnetization is oriented along the crystallographic easy axis so that the magnetocrystalline anisotropy energy does not explicitly appear in the free energy expression. The magnetic driving force for the variant reorietation is given by the *Zeeman energy* $-\mathbf{M}\cdot\mathbf{H}$, which describes the "misalignment" of the magnetic field with the magnetization in each variant.

In a two-dimensional configuration there exist only two tetragonal martensitic variants for the considered NiMnGa material and two possible orientations of the magnetization (i. e. two magnetic domains). The contribution of each to the total Gibbs free energy is incorporated by employing two nested, linearly weighted averages. A similar approach has been suggested in the literature.[13] In each averaging step the deviation of the total Gibbs free energy from the pure summation of the constituent contributions is accounted for by an additional mixing term.

$$\begin{aligned} G &= \hat{G}(T,\boldsymbol{\sigma},\mathbf{H},\xi,\boldsymbol{\varepsilon}^{\text{r}},\alpha) \\ &= G^{\text{V1}}(T,\boldsymbol{\sigma},\mathbf{H},\alpha) + \xi[G^{\text{V2}}(T,\boldsymbol{\sigma},\mathbf{H},\alpha) - G^{\text{V1}}(T,\boldsymbol{\sigma},\mathbf{H},\alpha)] \\ &\quad + G^{\xi\text{-mix}}(\xi,\boldsymbol{\varepsilon}^{\text{r}})\,, \end{aligned} \tag{8}$$

where, for each variant the contribution is given by

$$\begin{aligned} G^{\text{Vi}} &= \hat{G}(T,\boldsymbol{\sigma},\mathbf{H},\alpha) \\ &= G^{\text{mech,Vi}} + G^{\text{magn,Vi}} + G^{\alpha\text{-mix,Vi}} + G^{\text{th,Vi}} + G^{\text{ch,Vi}} \\ &= -\frac{1}{2\rho}\,\boldsymbol{\sigma}:\mathbf{S}^{\text{Vi}}\boldsymbol{\sigma} - \frac{1}{\rho}\,\boldsymbol{\sigma}:\boldsymbol{\alpha}^{\text{th,Vi}}(T-T_0) \\ &\quad - \frac{\mu_0}{\rho}[(1-\alpha)\mathbf{M}^{\text{Vi,D1}} + \alpha\mathbf{M}^{\text{Vi,D2}}]\cdot\mathbf{H} + G^{\alpha\text{-mix,Vi}} \\ &\quad + c\left[(T-T_0) - T\ln\left(\frac{T}{T_0}\right)\right] \\ &\quad + u_0 - Ts_0\,. \end{aligned} \tag{9}$$

Here, $\mathbf{S}^{\text{Vi}}$ denotes the elastic compliance tensor, $\boldsymbol{\alpha}^{\text{th,Vi}}$ the thermal expansion coefficient tensor of variant i. The scalar quantities heat capacity c, specific internal energy u_0 and specific entropy s_0 are the same in each variant. The subscript 0 indicates reference state values. It has been assumed that the density does not differ in the two martensitic variants since the reorientation process is volume conserving. The hardening behavior during the reorientation process is captured by the functions

$$\begin{aligned} G^{\alpha\text{-mix,Vi}} &= \frac{1}{\rho}\,f^{\alpha}(\alpha)\,, \\ G^{\xi\text{-mix}} &= \frac{1}{\rho}\,f^{\xi}(\xi,\boldsymbol{\varepsilon}^{\text{r}})\,. \end{aligned} \tag{10}$$

From the constitutive equations eqns. (5) these specific relations follow:

thermoelastic strain:

$$\boldsymbol{\varepsilon}^{\mathrm{te}} = -\rho\frac{\partial G}{\partial \boldsymbol{\sigma}} = \mathbf{S}\boldsymbol{\sigma} + \boldsymbol{\alpha}^{\mathrm{th}}(T - T_0) \,, \tag{11}$$

entropy:

$$s = -\frac{\partial G}{\partial T} = \frac{1}{\rho}\,\boldsymbol{\alpha}^{\mathrm{th}}\boldsymbol{\sigma} + c\ln\!\left(\frac{T}{T_0}\right) + s_0 \,, \tag{12}$$

where the abbreviations

$$\begin{aligned}\mathbf{S} &:= \mathbf{S}^{\mathrm{V1}} + \xi\Delta\mathbf{S} = \mathbf{S}^{\mathrm{V1}} + \xi(\mathbf{S}^{\mathrm{V2}} - \mathbf{S}^{\mathrm{V1}}) \,,\\ \boldsymbol{\alpha}^{\mathrm{th}} &:= \boldsymbol{\alpha}^{\mathrm{th,V1}} + \xi\Delta\boldsymbol{\alpha}^{\mathrm{th}} = \boldsymbol{\alpha}^{\mathrm{th,V1}} + \xi(\boldsymbol{\alpha}^{\mathrm{th,V2}} - \boldsymbol{\alpha}^{\mathrm{th,V1}}) \,,\end{aligned}$$

have been introduced for the averaged quantities.

magnetization:

With the possible magnitizations given by (cf. Figure 3)

$$\begin{aligned}\mathbf{M}^{\mathrm{V1,D1}} &= -M_s\mathbf{e}_x \,, \qquad \mathbf{M}^{\mathrm{V1,D2}} = M_s\mathbf{e}_x \,,\\ \mathbf{M}^{\mathrm{V2,D1}} &= -M_s\mathbf{e}_y \,, \qquad \mathbf{M}^{\mathrm{V2,D2}} = M_s\mathbf{e}_y \,,\end{aligned} \tag{13}$$

one obtains for the magnetization

$$\mathbf{M} = -\frac{\rho}{\mu_0}\,\frac{\partial G}{\partial \mathbf{H}} = -M_s(1-2\alpha)[(1-\xi)\mathbf{e}_x + \xi\mathbf{e}_y] \,. \tag{14}$$

thermodynamic driving forces:

With the individual local magnetization specified in eqns. (13) it follows for the *martensitic variant reorientation*

$$\begin{aligned}-\rho\frac{\partial G}{\partial \xi} &= \frac{1}{2}\,\boldsymbol{\sigma}:\Delta\mathbf{S}\boldsymbol{\sigma} + \boldsymbol{\sigma}:\Delta\boldsymbol{\alpha}^{\mathrm{th}}(T - T_0) + \mu_0(1-2\alpha)M_s[H_x - H_y]\\ &\quad - \rho\Delta c\left[(T - T_0) - T\ln\!\left(\frac{T}{T_0}\right)\right] - \rho\Delta u_0 + \rho T\Delta s_0 - \frac{\partial f^{\xi}}{\partial \xi} \,,\end{aligned} \tag{15}$$

and the *domain wall motion*

$$\begin{aligned}\pi^{\alpha} &:= -\rho\frac{\partial G}{\partial \alpha}\\ &= \mu_0\Big[[(1-\xi)(\mathbf{M}^{\mathrm{V1,D2}} - \mathbf{M}^{\mathrm{V1,D1}}) + \xi(\mathbf{M}^{\mathrm{V2,D2}} - \mathbf{M}^{\mathrm{V2,D1}})\Big]\cdot\mathbf{H} - \frac{\partial f^{\alpha}}{\partial \alpha}\\ &= 2\mu_0 M_s[(1-\xi)H_x + \xi H_y] - \frac{\partial f^{\alpha}}{\partial \alpha} \,,\end{aligned} \tag{16}$$

where eqns. (13) have again been used.

4.2. Evolution equations

The evolution of the macroscopic reorientation strain is assumed to be a function of the time rate of change of the martensitic variant volume fraction in the form of

$$\dot{\boldsymbol{\varepsilon}}^{\mathrm{r}} = \boldsymbol{\Lambda}^{\mathrm{r}} \dot{\xi} \, . \tag{17}$$

In the equation above $\boldsymbol{\Lambda}^{\mathrm{r}}$ is the reorientation strain tensor for which the explicit form will be presented for a special case in Section 5.1.

The integration of eqn. (17) leads to the reorientation strain. The total strain is then given by

$$\boldsymbol{\varepsilon} = \boldsymbol{\varepsilon}^{\mathrm{te}} + \boldsymbol{\varepsilon}^{\mathrm{r}} + \boldsymbol{\varepsilon}^{\mathrm{d}} = \mathbf{S}\boldsymbol{\sigma} + \boldsymbol{\alpha}^{\mathrm{th}}(T - T_0) + \boldsymbol{\Lambda}^{\mathrm{r}} \xi + \boldsymbol{\varepsilon}^{\mathrm{d}} \, , \tag{18}$$

and the Clausius-Duhem inequality (7) reduces to

$$\left[\boldsymbol{\sigma}^{\mathrm{eff}} : \boldsymbol{\Lambda}^{\mathrm{r}} - \rho \frac{\partial G}{\partial \xi} \right] \dot{\xi} - \rho \frac{\partial G}{\partial \alpha} \, \dot{\alpha} \geq 0 \, . \tag{19}$$

Or, with the definitions of thermodynamic driving forces conjugate to the internal variables ξ and α

$$\pi^{\xi} := \boldsymbol{\sigma}^{\mathrm{eff}} : \boldsymbol{\Lambda}^{\mathrm{r}} - \rho \frac{\partial G}{\partial \xi} \, , \quad \pi^{\alpha} := -\rho \frac{\partial G}{\partial \alpha} \, , \tag{20}$$

and considering the entropy input due to heat conduction separately, the Clausius-Duhem inequality can finally be written as

$$\pi^{\xi} \dot{\xi} + \pi^{\alpha} \dot{\alpha} \geq 0 \, . \tag{21}$$

The criterion for the onset of martensitic variant reorientation is given by

$$\pi^{\xi} = \pm Y^{\xi} \, , \tag{22}$$

where the plus sign is valid for the reorientation of variant 1 into variant 2 and the negative sign for the reverse process, respectively.

The hardening function for the variant reorientation is proposed to be

$$f^{\xi}(\xi) = \begin{cases} \frac{1}{2} A \xi^2 + (B_1 + B_2)\xi \, , & \dot{\xi} > 0 \\ \frac{1}{2} C \xi^2 + (B_1 - B_2)\xi \, , & \dot{\xi} < 0 \end{cases} \, . \tag{23}$$

The model is formulated generally enough to include the evolution of the magnetic domain volume fraction in a similar manner. However, the behavior of magnetic domains during the crystallographic reorientation process is not yet well understood and is subject of on going theoretical and experimental research. Even in materials that do not experience phase changes or mircostructural rearrangement, the magnetic domain distribution can be quite complicated. The size and structure of such domains are physically determined by the competition of energy terms such as the of magnetostatic, domain wall, magnetic anisotropy and elastic energies.[16,17] For the sake of simplicity the assumption $\alpha = 1.0$ is made in the current presentation of the model. This assumption has often been made in the literature and is in fact supported by reported observations that, after the application of relatively low magnetic fields ($> 100\,\mathrm{Oe} = 7.9\,\mathrm{kAm}^{-1}$), 180°-domain walls are essentially eliminated.[18]

5. APPLICATION OF THE CONSTITUTIVE MODEL.

With the general formulation of the model established we can now proceed to approach specific problems of technical interest. As described in Section 1 we aim to simulate and predict experimental results obtained from the set up depicted in Figure 2(a). Recall that the single crystal specimen is first biased into a single variant 1 state under a compressive axial load, which is kept constant during the experiment. With external application of the transverse magnetic field the crystal fully reorients into variant 2. This crystallographic reorientation process gives rise to the nonlinear macroscopic strain vs. magnetic field material response.

5.1. Reduced model equations

For the considered two-dimensional experiment certain simplifications apply. The specimen is being compressed along the x-axis. The external magnetic field is applied in the transverse y-direction resulting in the axial reorientation strain. The first term in eqn. (20) thus reduces to

$$\boldsymbol{\sigma}^{\mathrm{eff}} : \boldsymbol{\Lambda}^{\mathrm{r}} = \sigma_{xx}\varepsilon_{xx}^{\max} = \sigma\varepsilon^{\max} \; . \tag{24}$$

We further consider the experiment to be isothermal. For this case, using eqns. (15), (20) and (22) with the $\alpha = 1.0$ assumption, the conditions for the forward and the reverse reorientation process yield, respectively

reorientation $1 \rightarrow 2$ ($\dot{\xi} > 0$):

$$\pi^{\xi} = \sigma\varepsilon^{\max} + \frac{1}{2}\Delta S_{xx}\sigma^2 + \mu_0 M_s H_y - A\xi - B_1 - B_2 = Y^{\xi} \; . \tag{25}$$

Because of the scalar nature of the internal variable ξ eqn. (25) can be solved directly to give the closed-form solution for the evolution of the variant 2 volume fraction

$$\xi^{1\rightarrow 2} = \frac{1}{A}\left[\sigma\varepsilon^{\max} + \frac{1}{2}\Delta S_{xx}\sigma^2 + \mu_0 M_s H_y - B_1 - B_2 - Y^{\xi}\right] \; . \tag{26}$$

Similarly,

reorientation $2 \rightarrow 1$ ($\dot{\xi} < 0$):

$$\pi^{\xi} = \sigma\varepsilon^{\max} + \frac{1}{2}\Delta S_{xx}\sigma^2 + \mu_0 M_s H_y - C\xi - B_1 + B_2 = -Y^{\xi} \; , \tag{27}$$

and therefore

$$\xi^{2\rightarrow 1} = \frac{1}{C}\left[\sigma\varepsilon^{\max} + \frac{1}{2}\Delta S_{xx}\sigma^2 + \mu_0 M_s H_y - B_1 + B_2 + Y^{\xi}\right] \; . \tag{28}$$

5.2. Determination of material parameters of the model based on a phase diagram approach

The reorientation condition given by eqn. (22) can be graphically interpreted in terms of a phase diagram in axial biasing stress/transverse magnetic field space as seen in Figure 4. The depicted curves indicate the onset and termination of the forward ($H_s^{1,2}, H_f^{1,2}$) and reverse ($H_s^{2,1}, H_f^{2,1}$) reorientation process, respectively.

The shape and spacing of the reorientation start and finish lines is directly related to the parameters introduced with the hardening function eqn. (23) and the stress dependence of the maximum reorientation strain. For the so-called blocking stress σ_b the reorientation process is completely suppressed. The physical reason is that the elastic strain energy which has to be invested to align the long axes of the tetragonal unit cells of the crystal with the direction of the compressive load dominates the energetic gain from aligning the magnetization with the externally applied magnetic field.[‡] Here, the dependence of the maximum reorientation strain on the applied stress is approximated by a cubic polynomial

$$\varepsilon^{\max}(\sigma) = \varepsilon^{\max,0}\left[\left(\frac{\sigma}{\sigma_b}\right)^2 - 2\frac{\sigma}{\sigma_b} + 1\right] \; . \tag{29}$$

With an assumed slope of zero near the blocking stress the polynomial is uniquely defined by the blocking stress and the strain axis intercept (cf. Figure 5).

The six parameters A, C, B_1, B_2, Y^{ξ} and $\varepsilon^{\max,0}$, only five of which are independent, are directly determined by the acquisition of data from a single constant bias stress loop at an arbitrary stress level σ_p and the blocking

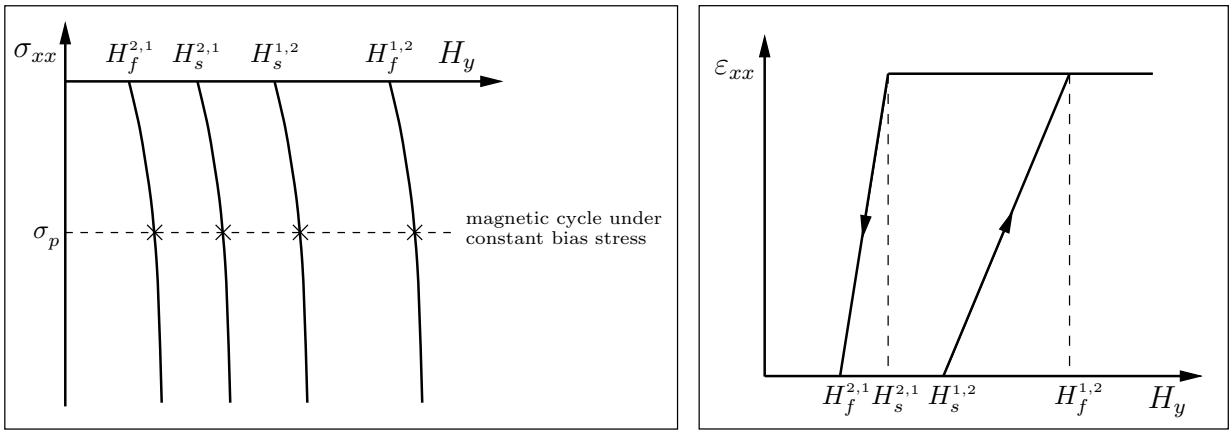

(a) Phase diagram for the variant reorientation process in MSMA. Displayed are the reorientation start and finish lines for the forward and reverse directions, respectively.

(b) Corresponding strain vs. magnetic field response for the cycle under constant stress bias.

Figure 4. Magnetic cycle under constant biasing stress.

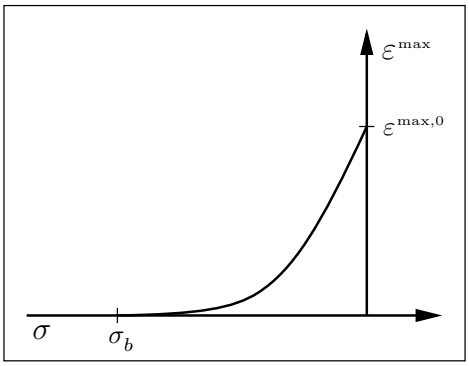

Figure 5. Schematic of the approximated dependence of the maximum reorientation strain on the applied axial stress.

stress, as indicated in Figure 4. The specific relations of the measured quantities to the model parameters are listed in Table 1.

A *Clausius-Clapeyron* type relation for the phase diagram can be deduced for example from eqn. (25)[§],

$$\frac{\mathrm{d}\sigma}{\mathrm{d}H_y} = -\frac{\mu_0 M_s}{\varepsilon^{\max} + \sigma \frac{\mathrm{d}\varepsilon^{\max}}{\mathrm{d}\sigma}} \ . \tag{30}$$

Note that in this model the stress dependence of the maximum reorientation strain is coupled to the curvature of the reorientation start and finish lines of the phase diagram.[¶]

[‡]One of the tasks of on going research is to find MSMA systems for which the blocking stress is high enough to build actuators. In NiMnGa single crystals for example the blocking stress is typically on the order of 10 Mpa or less.

[§]The difference in the x-component of the compliance is usually negligible.

[¶]Although the available data seems to support this approach, its physical accuracy certainly deserves further experimental investigation.

$$
\begin{aligned}
A &= \mu_0 M_s \big(H_2 - H_s^{1,2}(\sigma_p)\big) \\
B_1 &= \tfrac{1}{2}\mu_0 M_s \big(H_s^{1,2}(\sigma_p) + H_4\big) + \sigma_p\, \varepsilon^{\max}(\sigma_p) \\
B_2 &= \tfrac{1}{4}\mu_0 M_s \big(H_s^{1,2}(\sigma_p) - H_2 + H_3 - H_4\big) \\
C &= \mu_0 M_s \big(H_3 - H_4\big) \\
Y^{\xi} &= \tfrac{1}{2}\mu_0 M_s \big(H_s^{1,2}(\sigma_p) - H_4\big) - B_2 \\
\varepsilon^{\max,0} &= \big(\varepsilon^{\max}(\sigma_p)\, \sigma_b^2\big) / \big(\sigma_p - \sigma_b\big)^2
\end{aligned}
$$

Table 1. Relation of phase diagram and hardening parameters.

5.3. Results

As a numerical example let us consider the experiment based on data published by Tickle and James.[3,4] The experimental setup has been described in detail in Section 1. The material constants and model parameters for the considered NiMnGa single crystal magnetic shape memory alloy specimen are listed in Table 2 and have been found by applying the procedure described in Section 5.2.

μ_0	$1.256{\cdot}10^{-6}\,\mathrm{NA}^{-2}$
M_s	$0.622{\cdot}10^{6}\,\mathrm{Am}^{-1}$
ΔS_{xx}	$0.0\,\mathrm{Pa}^{-1}$
α	1.0
$H_s^{1,2}(\sigma_p)$	$3460{\cdot}79.6\,\mathrm{Am}^{-1}$
$H_f^{1,2}(\sigma_p)$	$12120{\cdot}79.6\,\mathrm{Am}^{-1}$
$H_s^{2,1}(\sigma_p)$	$5380{\cdot}79.6\,\mathrm{Am}^{-1}$
$H_f^{2,1}(\sigma_p)$	$760{\cdot}79.6\,\mathrm{Am}^{-1}$
σ_b	$-7.0\,\mathrm{MPa}$
$\varepsilon^{\max}(\sigma_p)$	0.0215

Table 2. Material constants and model parameters.

The resulting non-linear strain vs. magnetic field behavior is shown in Figure 6. This example demonstrates that the model captures all the important features of the reorientation process as far as the macroscopic straining of the material under applied magnetic fields is concerned. Namely, the dependence on the biasing stress level for the total reorientation strain, the slopes of the ε-H curves and the size of the hysteresis loop.[‖]

6. DISCUSSION

The results of Section 5.3 show that the specific form of the Gibbs free energy, in combination with the evolution equations and the phase diagram based transformation functions presented in Section 4, are adequate to model the ferromagnetic shape memory effect caused by the reorientation of martensitic variants. The main features

[‖] Note that the linearity of curves is due to the assumed form of the hardening functions (23), which can easily be modified.

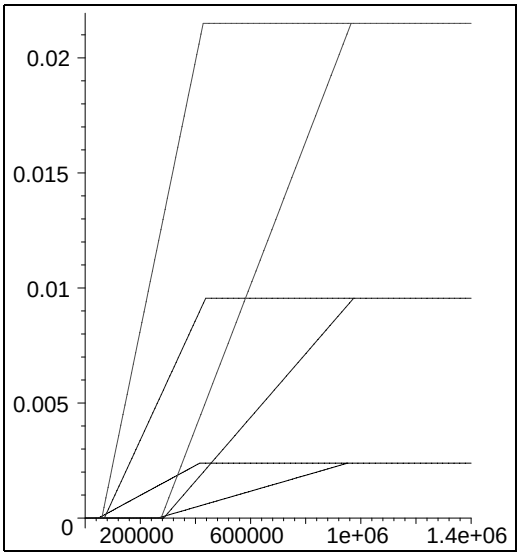

Figure 6. Axial reorientation strain vs. transversely applied magnetic field [Am^{-1}] for NiMnGa specimen at bias stress levels of -1 MPa, -3 MPa and -5 MPa.

of the constitutive behavior such as the biasing stress dependent change of shape of the hysteresis loops and the correct prediction of the onset and termination of the reorientation process are captured.

In a next step additional effects such as the possibility of rotation of the local magnetization away from the easy axis will be considered. The rotation of the magnetization, influences not only the macroscopic magnitization, it also reduces the driving force for twin boundary motion due to the Zeeman energy. Furthermore, the anisotropic magnetostriction effect, which may not be negligible in these materials, is coupled to the rotation of the local magnetization.[18,19] This will necessitate the explicit introduction of the magnetocrystalline anisotropy energy and magnetostriction into the free energy expression. The discussion about the importance of the magnetic microstructure, which some argue is essential while others deem it negligible, will also be addressed. As explained in Section 4.2 the model in general has the capacity to include the evolution of the magnetic domain structure. Experimental work currently performed in our group is trusted to support this effort. Other physical phenomena such as the influence of electromagnetic body forces or body couples, which, resolved onto the twin boundary plane, may have an effect on the twin boundary motion have been discussed in the literature[18] and will have to be addressed.

One has to note that most of the experimental data reported in the literature are based on work on single crystal specimen, although some work has also been done on polycrystalline materials.[2,20] In future work the model might therefore be taylored to include the anisotropic nature of the single crystalline materials more suitably. This effort would also include the generalization of the reorientation strain tensor to three-dimensional cases.

ACKNOWLEDGMENTS

This work was supported by the Army Research Office, contract no. DAAD 19-02-1-0261 and the National Science Foundation, award no. CMS-0324537. The authors would also like to acknowledge the inspiring discussion with Prof. O'Handley at the *SPIE Symposion on Smart Structures and Materials 2004* and his advice that is reflected mainly in the discussion section of this paper.

REFERENCES

1. H. E. Karaca, I. Karaman, D. C. Lagoudas, H. J. Maier, and Y. I. Chumlyakov, "Recoverable stress-induced martensitic transformation in a ferromagnetic CoNiAl alloy," *Scripta Materialia* **49**, pp. 831–836, 2003.
2. S. Jeong, K. Inoue, S. Inoue, K. Koterazawa, M. Taya, and K. Inoue, "Effect of magnetic field on martensite transformation in a polycrystalline Ni_2MnGa," *Material Science & Engineering A* **359**, pp. 253–260, 2003.
3. R. Tickle and R. D. James, "Magnetic and magnetomechanical properties of Ni_2MnGa," *Journal of Magnetism and Magnetic Materials* **195**(3), pp. 627–638, 1999.
4. R. Tickle, *Ferromagnetic Shape Memory Materials*. PhD thesis, University of Minnesota, May 2000.
5. R. Tickle. http://www.aem.umn.edu/people/others/tickle/.
6. K. Ullakko, J. K. Huang, C. Kantner, R. C. O'Handley, and V. V. Kokorin, "Large magnetic-field-induced strains in Ni_2MnGa single crystals," *Applied Physics Letters* **69**(13), pp. 1966–1968, 1996.
7. R. D. James and M. Wuttig, "Magnetostriction of martensite," *Philosophical Magazine A* **77**(5), pp. 1273–1299, 1998.
8. A. DeSimone and R. D. James, "A theory of magnetostriction oriented towards applications," *Journal of Applied Physics* **81**(8), pp. 5706–5708, 1997.
9. A. DeSimone and R. James, "A constrained theory of magnetoelasticity," *Journal of the Mechanics and Physics of Solids* **50**, pp. 283–320, 2002.
10. R. C. O'Handley, "Model for strain and magnetization in magnetic shape-memory alloys," *Journal of Applied Physics* **83**(6), pp. 3263–3270, 1998.
11. V. D. Buchelnikov and S. I. Bosko, "The kinetics of phase transformations in ferromagnetic shape memory alloys Ni-Mn-Ga," *Journal of Magnetism and Magnetic Materials* **258–259**, pp. 497–499, 2003.
12. A. A. Likhachev and K. Ullakko, "Magnetic-field-controlled twin boundaries motion and giant magneto-mechanical effects in Ni-Mn-Ga shape memory alloy," *Physics Letters A* **275**, pp. 142–151, 2000.
13. L. Hirsinger and C. Lexcellent, "Modelling detwinning of martensite platelets under magnetic and (or) stress actions on NiMnGa alloys," *Journal of Magnetism and Magnetic Materials* **254–255**, pp. 275–277, 2003.
14. B. D. Coleman and M. E. Gurtin, "Thermodynamics with internal state variables," *The Journal of Chemical Physics* **47**, pp. 597–613, July 1967.
15. B. D. Coleman and W. Noll, "The thermodynamics of elastic materials with heat conduction and viscosity," *Archive for Rational Mechanics and Analysis* **13**, pp. 167–178, 1963.
16. R. C. O'Handley, *Modern Magnetic Materials*, John Wiley & Sons, 2000.
17. C. Kittel, *Introduction to Solid State Physics*, John Wiley & Sons, 7th ed., 1996.
18. R. C. O'Handley, S. M. Allen, D. I. Paul, C. P. Henry, M. Marioni, D. Bono, C. Jenkins, A. Banful, and R. Wager, "Keynote address: Magnetic field-induced strain in single crystal Ni-Mn-Ga," *Proceedings of SPIE* **5053**, pp. 200–206, 2003.
19. R. C. O'Handley, "Privat technical discussion." SPIE, 11th Annual International Symposium: Smart Structures and Materials, San Diego, CA., 14–18 March 2004.
20. T. Wada, Y. Liang, H. Kato, T. Tagawa, M. Taya, and T. Mori, "Structural change and straining in Fe-Pd polycrystals by magnetic field," *Material Science & Engineering A* **361**, pp. 75–82, 2003.
21. Y. H. Pao and K. Hutter, "Electrodynamics for moving elastic solids and viscous fluids," *Proceedings of the IEEE* **63**(7), pp. 1011–1021, 1975.
22. L. E. Malvern, *Introduction to the Mechanics of a Continuous Medium*, Series in Engineering of the Physical Sciences, Prentice Hall, 1969.
23. C. Truesdell and R. Toupin, *Principles of Classical Mechanics and Field Theory*, vol. III/1 of *Encyclopedia of Physics*, ch. The Classical Field Theories, pp. 226–795. Springer-Verlag, 1960.
24. K. Hutter and A. A. F. van de Ven, *Field Matter Interactions in Thermoelastic Solids*, vol. 88 of *Lecture Notes in Physics*, Springer-Verlag, 1978.